PROCEEDINGS OF SCIENCE

Hadron spectroscopy and hadron-hadron interactions

Paolo Gandini[a,*]
on behalf of the ATLAS, CMS, ALICE and LHCb collaborations
[a] *Istituto Nazionale di Fisica Nucleare, Milan, Italy*
E-mail: paolo.gandini@mi.infn.it

These proceedings present a selection of results on behalf of all the experiments at LHC. This contribution covers a selection of results appeared after the 2024 winter conferences and before ICHEP2024. Highlights include the observation of new charmonium(-like) states in $B^+ \to D^{*\pm} D^{\mp} K^+$ decays and exotic $J/\psi\phi$ resonances produced in central exclusive production collisions. Additionally, the Elliptic anisotropy measurement of the f0(980) hadron in proton-lead collisions at CMS is described, along with a similar analysis by the ALICE experiment on the observation of abnormal suppression of f0(980) production in p-Pb collisions. The analyses presented are:

- LHCb: Observation of new charmonium(-like) states in $B^+ \to D^{*\pm} D^{\mp} K^+$ decays.
- LHCb: Observation of exotic $J/\Psi\phi$ resonances in CEP collisions.
- LHCb: Search for P_c pentaquarks in open charm modes.
- CMS: Observation of the $\Xi_b \to \Psi(2S)\Xi$ decay and studies of the Ξ_b^* baryon.
- CMS: Elliptic anisotropy measurement of the f0(980) hadron in proton-lead collisions.
- ALICE: Observation of abnormal suppression of f0(980) production in p-Pb collisions.

12th Large Hadron Collider Physics Conference (LHCP2024)
3-7 June 2024
Boston, USA

*Speaker

PoS(LHCP2024)166

1. Introduction: QCD

QuantumChromo Dynamics (QCD) describes the behaviour of strong interacting particles. However, understanding the non-perturbative property of QCD at low-energy scales is still an open and active research field. In this respect, the spectroscopy of heavy hadrons provides an important tool to probe the low-energy regimes (see Fig.1 for a pictorial view). In recent years, heavy quark spectroscopy has been subject to continuous advances both experimentally and theoretically. So far more than 72 hadrons have been discovered at the LHC as shown in Fig.2, with all the main experiments contributing. The list is growing at a steady pace and with more data becoming available in the upgrade area, further observations could be expected.

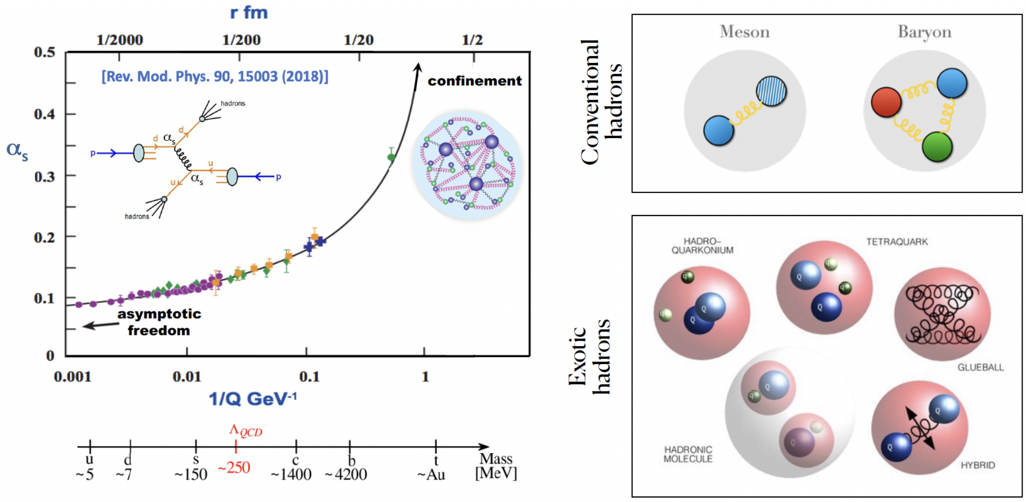

Figure 1: Pictorial view of QCD at different energy regimes. An overview of the currently observed hadrons is also presented on the right.

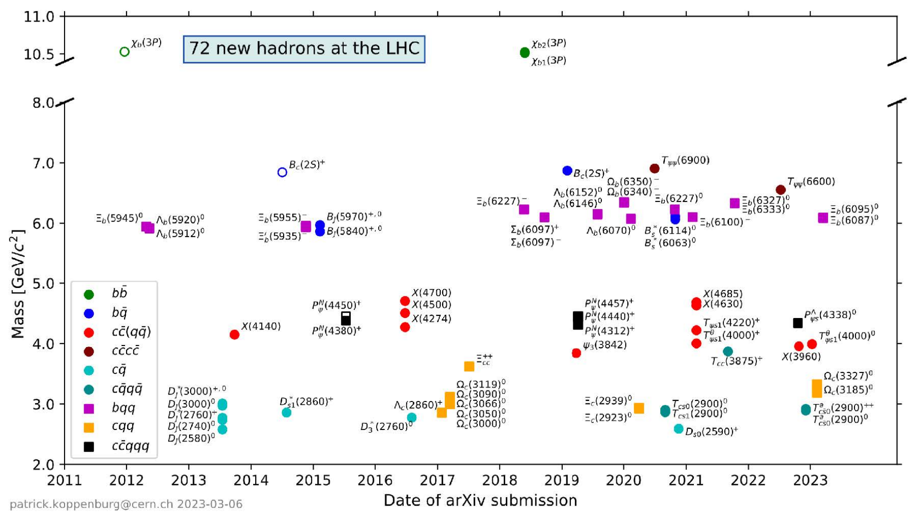

Figure 2: List of the new hadrons observed at the LHC at the time of writing [1].

2. LHCb: Observation of new charmonium(-like) states in $B^+ \to D^{*\pm} D^{\mp} K^+$ decays [2]

A study of possible resonant structures in $B^+ \to D^{*+} D^- K^+$ and $B^+ \to D^{*-} D^+ K^+$ decays is presented. The mass distributions of these decays are shown in Fig.3. A simultaneous amplitude fit is performed to the two channels including contributions from resonances decaying to $D^{*-}D^+$ and $D^{*+}D^-$ states (linked by C parity). The C parity of any new state is determined and it is shown in Fig.4. Four charmonium(-like) states are observed decaying into $D^{*\pm}D^{\mp}$: $\eta_c(3945)$, $h_c(4000)$, $\chi_{c1}(4010)$ and $h_c(4300)$, with quantum numbers J^{PC} equal to 0^{-+}, 1^{+-}, 1^{++} and 1^{+-}, respectively. At least three of these states have not been observed previously. In addition, the existence of the $T^*_{\bar{c}\bar{s}0}(2870)^0$ and $T^*_{\bar{c}\bar{s}1}(2900)^0$ resonances in the D^-K^+ mass spectrum, already observed in the $B^+ \to D^+ D^- K^+$ decay, is confirmed in a different production channel.

PoS(LHCP2024)166

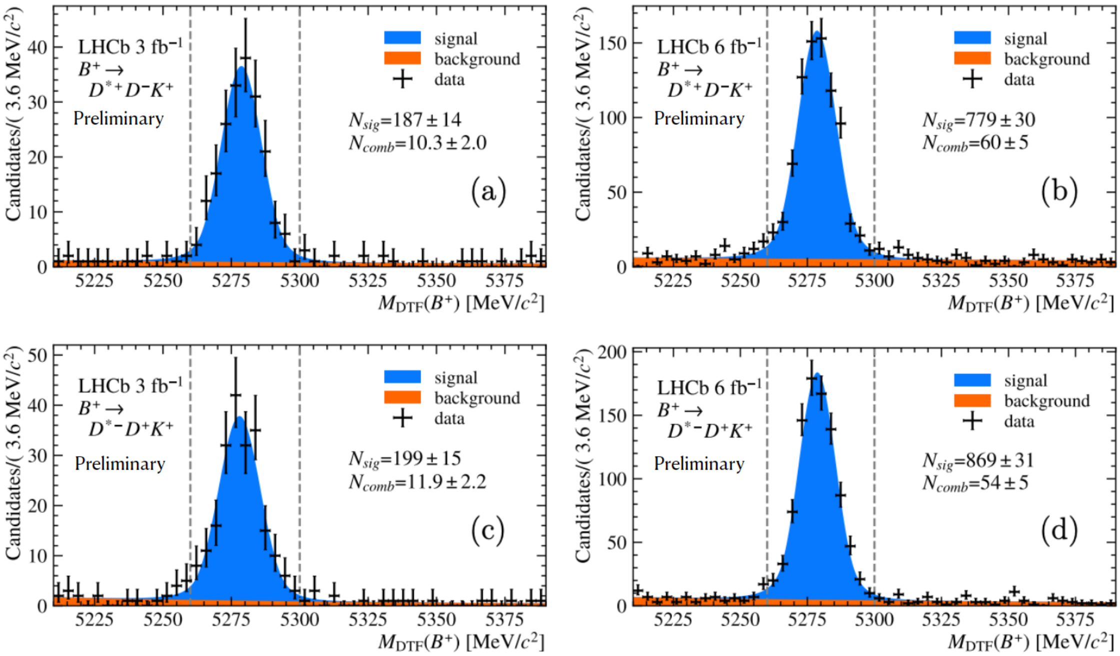

Figure 3: Mass distributions for $B^+ \to D^{*+} D^- K^+$ and $B^+ \to D^{*-} D^+ K^+$ decays.

3. LHCb: Observation of exotic $J/\Psi\phi$ resonances in CEP collisions [3]

The first study of $J/\Psi\phi$ production in diffractive processes in proton-proton collisions is presented. The study is based on an LHCb dataset recorded at centre-of-mass energy of 13 TeV, corresponding to an integrated luminosity of 5 fb^{-1}. Central Exclusive Production (CEP) consists of inelastic events where the protons remain intact, with the production of low p_T objects, as shown in Fig.5. The data disfavour a non-resonant $J/\Psi\phi$ production but are consistent with models including several resonant states observed previously only in B decays (see Fig.6). In particular, the $\chi_{c0}(4500)$ state is observed with a significance over 5 σ and the $\chi_{c1}(4274)$ is confirmed with a significance of more than 4 σ.

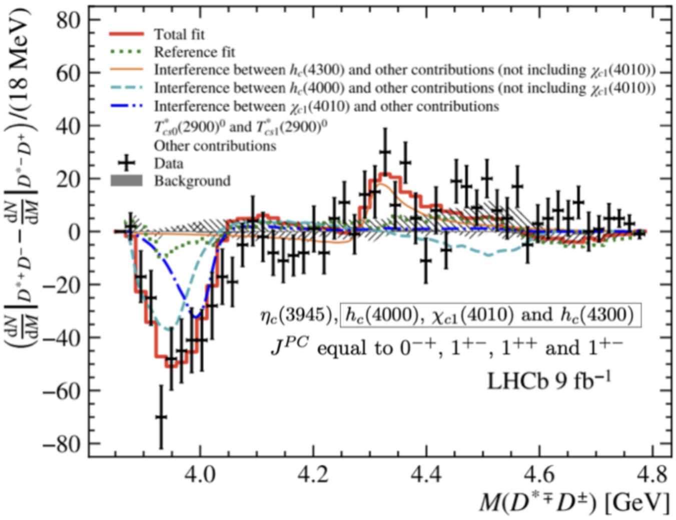

Figure 4: Distributions of two-body invariant masses: (a) $M(D^{*-}D^+)$, (c) $M(D^+K^+)$ and (e) $M(D^{*-}K^+)$ in the $B^+ \to D^{*-}D^+K^+$ sample; (b) $M(D^+D^-)$, (d) $M(D^-K^+)$ and (e) $M(D^{*+}K^+)$ in the $B^+ \to D^{*+}D^-K^+$ sample. The fit results (red-solid lines) are overlaid on the data distributions. Contributions from different components are also shown in different line styles as indicated in the legend. The result of fitting the data using a model without the $h_c(4000)$, $\chi_{c1}(4010)$ and $h_c(4300)$ components (reference fit) is shown with green-dotted lines for comparison.

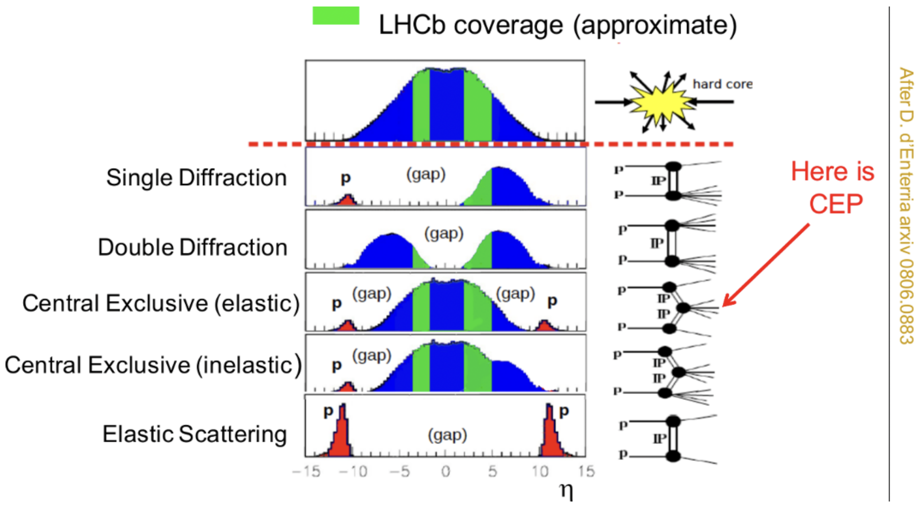

Figure 5: A pictorial view of elastic and inelastic processes in proton-proton collisions.

4. LHCb: Search for P_c pentaquarks in open charm modes [4]

An inclusive search for hidden-charm pentaquark states is presented using 5.7 fb^{-1} data from 2016-2018. The analysis uses a range of $\Sigma_c\bar{D}$ and $\Lambda_c^-\bar{D}$ final states, as well as doubly-charmed pentaquark states decaying to $\Sigma_c D$ and $\Lambda_c^+ D$, as shown in Fig.7. Since no significant signals are found, upper limits are set on the pentaquark yields relative to that of the Λ_c^+ baryon. The known pentaquark states are also investigated, and their signal yields are found to be consistent with zero

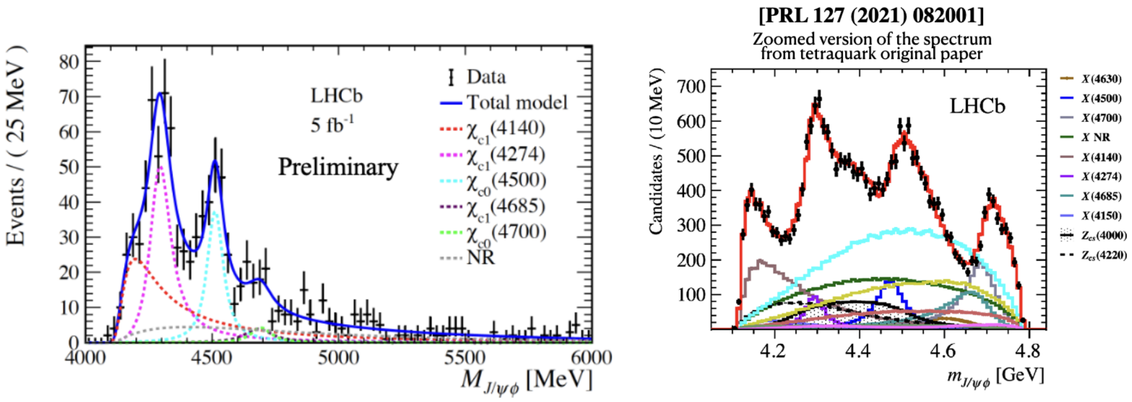

Figure 6: Left: $J/\Psi\phi$ mass spectrum and its interesting resonant contributions. Right: a zoomed version of the same spectrum from the tetraquark paper.

hidden-charm pentaquarks

Hadron 1	Hadron 2	Charge	I_3	Y	C	Limit Set
Λ_c^+	$\overline{D}^0$	+1	$1/2$	1	0	✓
Λ_c^+	D^-	0	$-1/2$	1	0	✓
Λ_c^+	D^{*-}	0	$-1/2$	1	0	✓
Σ_c^{++}	$\overline{D}^0$	+2	$3/2$	1	0	✓
Σ_c^{++}	D^-	+1	$1/2$	1	0	✓
Σ_c^{++}	D^{*-}	+1	$1/2$	1	0	×
Σ_c^{0}	$\overline{D}^0$	0	$-1/2$	1	0	✓
Σ_c^{0}	D^-	−1	$-3/2$	1	0	✓
Σ_c^{0}	D^{*-}	−1	$-3/2$	1	0	×
Σ_c^{*++}	$\overline{D}^0$	+2	$3/2$	1	0	✓
Σ_c^{*++}	D^-	+1	$1/2$	1	0	✓
Σ_c^{*++}	D^{*-}	+1	$1/2$	1	0	✓
Σ_c^{*0}	$\overline{D}^0$	0	$-1/2$	1	0	✓
Σ_c^{*0}	D^-	−1	$-3/2$	1	0	✓
Σ_c^{*0}	D^{*-}	−1	$-3/2$	1	0	✓

doubly-charmed pentaquarks & excited Ξ_{cc}

Hadron 1	Hadron 2	Charge	I_3	Y	C	Limit Set
Λ_c^+	D^0	+1	$-1/2$	3	2	✓
Λ_c^+	D^+	+2	$1/2$	3	2	✓
Λ_c^+	D^{*+}	+2	$1/2$	3	2	✓
Σ_c^{++}	D^0	+2	$1/2$	3	2	×
Σ_c^{++}	D^+	+3	$3/2$	3	2	×
Σ_c^{++}	D^{*+}	+3	$3/2$	3	2	×
Σ_c^{0}	D^0	0	$-3/2$	3	2	×
Σ_c^{0}	D^+	+1	$-1/2$	3	2	×
Σ_c^{0}	D^{*+}	+1	$-1/2$	3	2	×
Σ_c^{*++}	D^0	+2	$1/2$	3	2	✓
Σ_c^{*++}	D^+	+3	$3/2$	3	2	✓
Σ_c^{*++}	D^{*+}	+3	$3/2$	3	2	×
Σ_c^{*0}	D^0	0	$-3/2$	3	2	✓
Σ_c^{*0}	D^+	+1	$-1/2$	3	2	✓
Σ_c^{*0}	D^{*+}	+1	$-1/2$	3	2	×

10 modes too statistically limited to set up upper limits

Figure 7: List of the baryon combinations considered in the analysis.

in all cases. The results with the corresponding limits are presented in Fig.8.

5. CMS: Observation of the $\Xi_b \to \Psi(2S)\Xi$ decay and studies of the Ξ_b^* baryon [5]

The first observation of the decay $\Xi_b \to \Psi(2S)\Xi$ is presented along with its branching fraction measurement with respect to the known $\Xi_b \to J\Psi\Xi$ mode. The results are based on proton-proton colliding beam data from the LHC collected by the CMS experiment at $\sqrt{s} = 13$ TeV in 2016–2018 corresponding to an integrated luminosity of 140 fb^{-1}. New measurements of the Ξ_b^{*0} baryon mass and natural width are also presented. Results are summarized in Fig.9.

$$R = \frac{N_{P_c}}{N_{\Lambda_c^+}} \times \frac{\varepsilon_{\Lambda_c^+}}{\varepsilon_{P_c}} \rightarrow \frac{\sigma(P_c)\times\mathcal{B}\left(P_c\rightarrow\Lambda_c^+ D(\pi)\right)\times\mathcal{B}(D)}{\sigma(\Lambda_c^+)}$$

Decay Mode	Width (MeV/c^2)	Significance (σ) Local	Corrected	Q-value (MeV/c^2)	Signal Yield	UL ($\times 10^{-3}$) 90% CL	95% CL
$\Lambda_c^+\pi^+D^-$	0	3.59	2.21	225	41.6 ± 12.6	3.95	4.19
	5	4.01	2.89	225	64.7 ± 17.4	4.43	4.69
	10	4.30	3.32	225	87.1 ± 21.6	4.64	4.85
	15	4.50	3.62	225	108.2 ± 25.3	4.72	4.90
$\Lambda_c^+\pi^-D^-$	0	3.36	1.90	257	38.1 ± 12.4	4.28	4.56
	5	3.86	2.71	253	62.1 ± 17.1	4.62	4.83
	10	4.18	3.20	249	83.7 ± 21.2	4.72	4.88
	15	4.44	3.56	249	103.5 ± 24.6	4.77	4.92
$\Lambda_c^+\pi^+\overline{D}^0$	0	3.18	1.58	245	41.9 ± 13.7	2.87	3.06
	5	3.73	2.53	245	67.6 ± 19.2	3.22	3.35
	10	4.06	3.06	245	91.6 ± 24.1	3.29	3.39
	15	4.30	3.42	245	115.0 ± 28.5	3.30	3.40

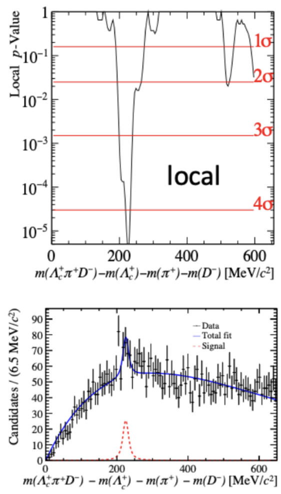

Figure 8: Yields and calculated upper limits for each mode.

Decay channel	N	$m^{\mathrm{fit}}_{\Xi_b^-}$ (MeV)	σ_{eff} (MeV)
$\Xi_b^- \rightarrow \mathrm{J}/\psi\Xi^-$	846 ± 40	5797.1 ± 0.6	16.3 ± 1.0
$\Xi_b^- \rightarrow \mathrm{J}/\psi\Lambda\mathrm{K}^-$	920 ± 98	5798.8 ± 0.9	11.9 ± 1.5
$\Xi_b^- \rightarrow \mathrm{J}/\psi\Sigma^0\mathrm{K}^-$	880 ± 170	—	—
$\Xi_b^- \rightarrow \psi(2S)\Xi^-$ (with $\psi(2S)\rightarrow\mu^+\mu^-$)	74 ± 11	5797.7 ± 1.4	11.1 ± 2.0
$\Xi_b^- \rightarrow \psi(2S)\Xi^-$ (with $\psi(2S)\rightarrow \mathrm{J}/\psi\pi^+\pi^-$)	90 ± 14	5797.2 ± 1.7	13.1 ± 2.8

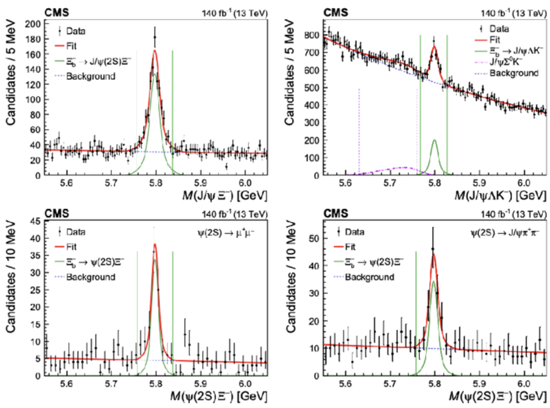

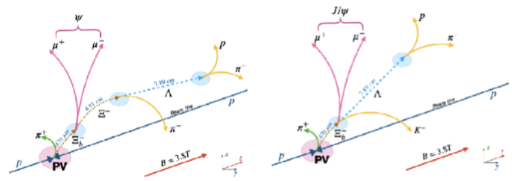

$$R_{\Xi_b^{*0}} = \frac{\sigma(\mathrm{pp}\rightarrow\Xi_b^{*0}X)\,\mathcal{B}(\Xi_b^{*0}\rightarrow\Xi_b\pi^+)}{\sigma(\mathrm{pp}\rightarrow\Xi_b X)} = 0.23 \pm 0.04\,(\mathrm{stat}) \pm 0.02\,(\mathrm{syst})$$

$$R = \frac{\mathcal{B}(\Xi_b^- \rightarrow \psi(2S)\Xi^-)}{\mathcal{B}(\Xi_b^- \rightarrow \mathrm{J}/\psi\Xi^-)} = 0.84^{+0.21}_{-0.19}\,(\mathrm{stat}) \pm 0.10\,(\mathrm{syst}) \pm 0.02\,(\mathcal{B})$$

$$M(\Xi_b^{*0}) = 5952.4 \pm 0.1\,(\mathrm{stat{+}syst}) \pm 0.6\,(m_{\Xi_b^-})\ \mathrm{MeV}$$

Figure 9: Summary of the results presented in the paper.

6. CMS: Elliptic anisotropy measurement of the f0(980) hadron in proton-lead collisions [6]

The f0(980) hadron discovered half a century ago, but its quark content has not been settled with several options on its nature still standing (ordinary meson, tetraquark, exotic state, $K\bar{K}$ molecule, hybrid). This paper reports strong evidence that f0(980) is an ordinary meson, inferred from scaling of elliptic anisotropies (v_2), with the number of constituent quarks (n_q). The f0(980) state is reconstructed via its dominant decay channel $\pi^+\pi^-$, in proton-lead collisions recorded by the CMS experiment at the LHC and its v_2 is measured as a function of transverse momentum. The hypothesis of conventional $q\bar{q}$ meson is empirically established using conventional hadrons in relativistic heavy ion collisions, while other hypotheses on its exotic nature are ruled out (see

Fig.10. This result represents the first determination of the quark content of the f0(980) state, made

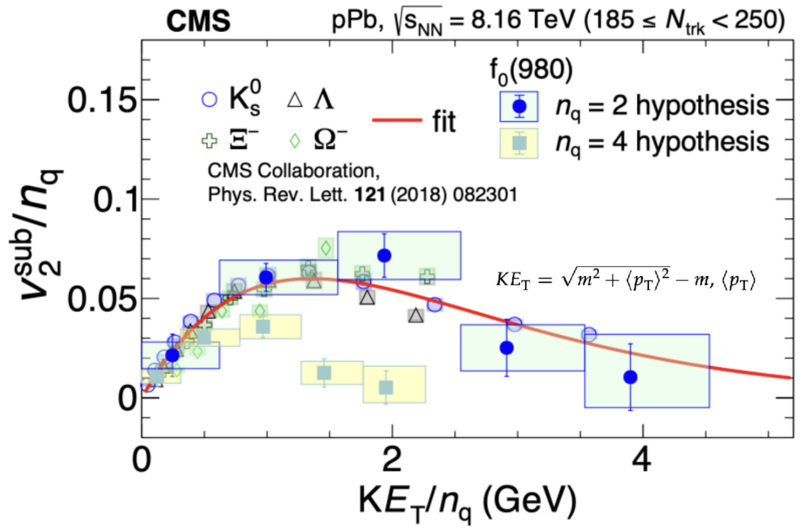

The argument of the function, KE_T/n_q, is related to the kinetic energy per constituent quark

Figure 10: NCQ scaling of elliptic anisotropy. The v_2 of the f0 state (for the $n_q = 2$ and 4 hypotheses) compared with different hypotheses.

possible by using a novel approach, and paves the way for similar studies of other exotic hadron candidates.

7. ALICE: Observation of abnormal suppression of f0(980) production in p-Pb collisions [7]

The nuclear modification factor QpPb of f0(980) measured in various multiplicity ranges. The dependence of $f_0(980)$ production on the final-state charged-particle multiplicity in p–Pb collisions at $\sqrt{s_{NN}} = 5.02$ TeV is investigated. The production of $f_0(980)$ is measured with the ALICE detector via the $f_0(980) \to \pi^+\pi^-$ decay channel in a midrapidity region of $-0.5 < y < 0$. Particle yield ratios of $f_0(980)$ to π and $K^*(892)^0$ are found to be decreasing with increasing charged-particle multiplicity. The magnitude of the suppression of the $f_0(980)/\pi$ and $f_0(980)/K^*(892)^0$ yield ratios is found to be dependent on the transverse momentum p_T, suggesting different mechanisms responsible for the measured effects. Furthermore, the nuclear modification factor Q_{pPb} of $f_0(980)$ is measured in various multiplicity ranges. The Q_{pPb} shows a strong suppression of the $f_0(980)$ production in the p_T region up to about 4 GeV/c. The results on the particle yield ratios may help to understand the nature of the internal structure of f0(980) particle. A snapshot of the main results is shown in Fig.11.

References

[1] The LHCb collaboration., Koppenburg, P. List of hadrons observed at the LHC, LHCb-FIGURE-2021-001, 2021, and 2023 updates. LHCb-FIGURE-2021-001, 2021, and 2024 updates.

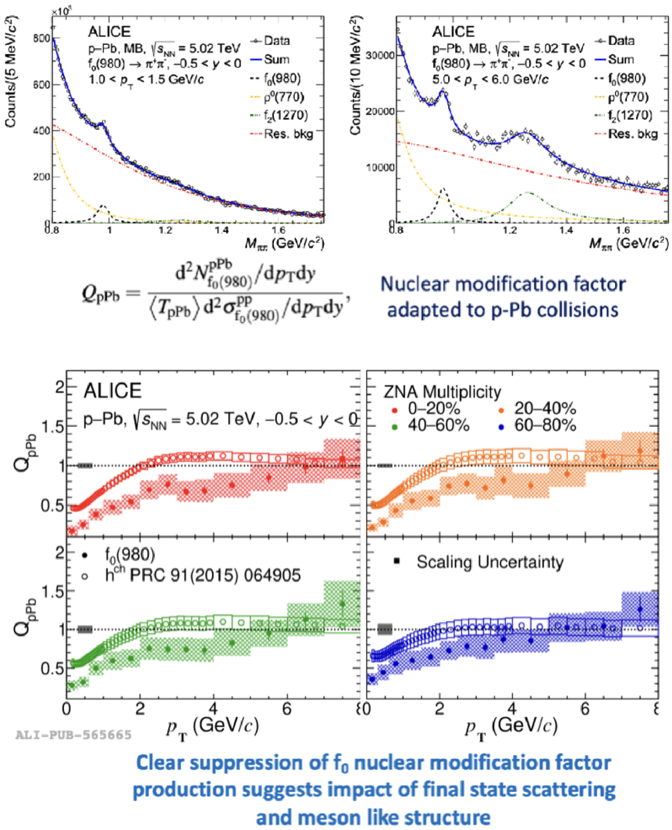

Figure 11: Summary of the results presented in paper [7]

[2] The LHCb collaboration., Aaij, R., et al. Observation of new charmonium or charmonium-like states in $B^+ \to D^{*\pm}D^{\mp}K^+$ decays Phys. Rev. Lett. 133, 131902.

[3] The LHCb collaboration., Aaij, R., et al. Observation of exotic $J/\Psi\phi$ resonances in diffractive processes in proton-proton collisions. arXiv:2407.14301.

[4] The LHCb collaboration., Aaij, R., et al. Search for prompt production of pentaquarks in charm hadron final states. Phys. Rev. D 110 (2024) 032001

[5] The CMS collaboration., Hayrapetyan, A., et al. Observation of the $\Xi_b \to \Psi(2S)\Xi$ decay and studies of the Ξ_b^* baryon. Phys. Rev. D 110, 012002

[6] The CMS collaboration., Hayrapetyan, A., et al. Elliptic anisotropy measurement of the f0(980) hadron in proton-lead collisions and evidence for its quark-antiquark composition. Submitted to Nature Physics

[7] The ALICE collaboration., Acharya, S., et al. Observation of abnormal suppression of f0(980) production in p–Pb collisions at $\sqrt{s_{NN}}$ = 5.02 TeV. Phys. Lett. B 853 (2024) 138665